The Influence of Different Treatments of Electrostatic Interactions on the Thermodynamics of Folding of Peptides†

Andrij Baumketner‡ and Joan-Emma Shea*

Department of Chemistry and Biochemistry, University of California at Santa Barbara, Santa Barbara, California 93106

Received: March 14, 2005

Replica exchange molecular dynamics simulations were performed to investigate the effects of different electrostatic treatments on the structure and thermodynamics of a small β-hairpin forming peptide. Three different electrostatic schemes were considered: regular cutoffs, generalized reaction field (GRF), and particle mesh Ewald (PME), with the peptide modeled using OPLS/AA all-atom force field with explicit TIP3P water. Both the GRF and PME methods yielded results consistent with experiment, with free energy surfaces displaying a single minimum corresponding to the native β-hairpin structure. In contrast, use of straight cutoffs led to the population of an additional local minimum corresponding to nonhairpin conformations that compete with the formation of the native β-hairpin at low temperatures. This extra minimum would not be apparent in conventional constant-temperature molecular dynamics simulations run for a few nanoseconds. This result points to the critical need of careful sampling of conformational space to assess the quality of different numerical treatments of long-range forces. While differences emerged in the nature of the unfolded states populated using PME and GRF approaches, simulations on the β-hairpin forming peptide and on two additional control peptides indicate that the GRF treatment of electrostatics offers a satisfactory compromise between accuracy and computational speed for the identification of low-energy conformations. A GRF-based approach emerges as a viable means for treating larger biological systems that would be prohibitively costly to simulate using PME methods.

1. Introduction

Microscopic fully atomic molecular dynamics simulations are playing an increasingly important role in the theoretical investigations of biological molecules.[1−6] The success of numerical approaches depends critically on their accuracy, and there are several well-known sources of errors plaguing these simulations. These include, among others, (i) a classical approximation that neglects electronic degrees of freedom and treats atoms as single interacting centers, (ii) a possibly inadequate parametrization and nontransferability of force fields, (iii) artifacts due to periodic boundary conditions, and finally (iv) the treatment of electrostatics.

Of the four sources of errors described above, the treatment of the electrostatic interactions is the most critical to achieve accuracy in simulations.[7,8] Indeed, the classical approximation seems to be a reasonable one for large biomolecules, and modern force fields appear to be adequate for simulations of biomolecules ranging from globular proteins[1,2,9] to di-and tripeptide systems[10−12] to amino acid analogues.[13] Artifacts due to periodic boundary conditions, such as the over-stabilization of certain conformational states, can be largely eliminated by increasing the size of the simulation box.[14]

The proper treatment of long-range interactions has been an active field of research for the past two decades.[15,16] Initial studies focused on the solvation of single ions in aqueous solutions and on the determination of the potential of mean force (PMF) of pairs of ions (see ref 14 and references therein), yielding critical information regarding ion solvation energies, and preferred ion−ion distances. Later work sought to investigate more directly the effect of various treatments of electrostatic interactions on a number of peptides,[16−19] proteins,[15,20−25] and oligonucleotides[22,26] of known three-dimensional structure. Methods used to treat electrostatics of biomolecules include both simplified "cutoff" methods in which the long-range interactions are truncated beyond a certain distance, as well as more sophisticated cutoff approaches (including Onsager and generalized reaction field methods). In the latter, the interactions of the molecule inside a sphere of radius given by the cutoff distance are calculated explicitly, and the environment outside this sphere is modeled by a homogeneous medium of a given dielectric constant. These continuum-based reaction field approaches, although approximate, have the advantage of computational efficiency, an essential element for the study of large biomolecular systems. More accurate (and significantly more costly) noncutoff-based methods include Ewald and particle-mesh Ewald approaches. Simulations testing the accuracy of the above methods have typically started from solvated native conformations (obtained from NMR or crystallographic data) and were run for several nanoseconds to determine the extent to which the system would deviate from the initial state. Although these studies provided valuable insight into the stability of the native state and the degree of structural fluctuations around it, they present the serious drawback of uniquely focusing on the narrow region of conformational space located near the known initial structure. Even the longest

† Part of the special issue "Irwin Oppenheim Festschrift".

* To whom correspondence should be addressed: E-mail: shea@chem.ucsb.edu.

‡ Permanent address: Institute for Condensed Matter Physics, 1 Svientsitsky Str., Lviv 79011, Ukraine. E-mail: andrij@icmp.lviv.ua.

10.1021/jp051325a CCC: $30.25
Published on Web 06/28/2005

simulation time recently reported (a 500 ns run by Colombo et al.[16]) is not sufficient to permit a full exploration of conformational space and to allow transitions into other structures of relevance at the given temperature of the simulation. As a result, only the native-state minimum will be sampled, and any minima, other than the native one, that may be introduced through approximate electrostatic treatments will not be seen in such simulations. To gain a true understanding of the influence of electrostatic treatments on simulations of biomolecules, it is hence imperative to use sampling techniques capable of providing a *global* coverage of available conformational space and not uniquely the *local* area near the known structure. This becomes even more critical in situations where the low-energy states of peptides are not known and are to be identified through simulation, or for simulations aiming at testing the accuracy of force field parameters. An enhanced sampling protocol will be essential to ensure that the tested force field parameters are not only capable of folding the molecule into the intended structure but, equally importantly, that they do not introduce artifacts that lead to folding into additional non-native states.

To our knowledge, there have been no systematic studies investigating the effects of electrostatic treatments on the entire conformational space that a peptide can sample. The aim of this paper is to address this matter by using enhanced sampling replica exchange molecular dynamics to study the influence of three commonly used methods, regular cutoffs, particle mesh Ewald method (PME),[27] and generalized reaction field (GRF) method[28] on the structure and thermodynamics of a β-hairpin forming peptide. A key question will be to determine whether the GRF method, significantly less costly that the PME, has sufficient accuracy to be used for the study of protein and peptide folding. While PME methods are tractable for peptides, they become rapidly prohibitively costly for even the smallest proteins. It is hence critical to identify a treatment of electrostatics that is efficient yet does not sacrifice accuracy to probe the thermodynamics of folding.

The main subject of our study is the hairpin-forming peptide YQNPDGSQA designed by Blanco et al.[29] This peptide has been studied experimentally by Constantine, Friedrichs et al.[30,31] using NMR as well as computationally through short constant temperature simulations by Constantine et al.[32] and Brooks et al.[33,34] Our replica exchange simulations employ a fully atomic description of the peptide using the OPLS/AA[35] all-atom empirical force field together with explicit TIP3 water molecules.[36] Free energy surfaces, projected onto the first two principal components, are generated using each electrostatic scheme. The quality of a given electrostatic treatment is assessed from these surfaces, a key criterion being that the numerical scheme should fold the peptide into its native β hairpin, and only into this native state, and that this be the lowest free energy state.

All three electrostatic schemes tested are seen to be able to find the correct native state corresponding to the experimentally determined β-hairpin. However, only the PME- and GRF-based schemes have free energy surfaces exhibiting a single, global minimum. In contrast, the free energy map generated using a simple cutoff displays an additional nonhairpin minimum of energy comparable to that of the native β-hairpin. Differences emerge in the nature of the unfolded state sampled in the PME- and GRF-simulations, but as a whole, both these methods are in good agreement and yield the unique native state found in experiment. Additional simulations were run on two control peptides, YQSWRYSQA and GHNPDGHG-NH_2, to further validate the use of GRF methods as both an efficient and accurate protocol for simulations of larger biomolecular systems.

2. Models and Methods

Three peptides were investigated in this work, a main peptide and two control peptides. All three peptides were described by the all-atom OPLS/AA[35] force field and solvated in cubic boxes with TIP3P water molecules,[36] under periodic boundary conditions. The sizes of the simulation boxes were determined from short constant pressure simulations at $T = 280$ K, equilibrated at a physiological external pressure of 1 atm. The first peptide studied, the main subject of this investigation, is the YQNPDGSQA peptide, a mutant of the 15−23 fragment of the α-amylase inhibitor Tendamistat (PDB code 1HOE), in which the original SWRY segment was replaced by the NPDG sequence. The resulting peptide[29] exhibited NOEs compatible with those of a β-hairpin structure. Under neutral pH conditions, this peptide has a −1 total electrical charge, due to the presence of titratable residues and terminal groups. This charge was neutralized in our simulations by addition of one sodium counterion. The simulation box used was 33.1 Å, with 1149 water molecules and a total of 3574 atoms The second peptide studied (control peptide 1) is the wild-type 15−23 fragment of the α-amylase inhibitor Tendamistat (YQSWRYSQA). A simulation box of 35 Å, with 1346 water molecules and a total number of 4198 atoms was used. One chlorine −1 counterion was introduced to cancel the net +1 charge of the peptide. The final peptide (control peptide 2), GHNPDGHG-NH_2 was simulated in a box of 33 Å with 1150 water molecules and 3550 total atoms. No additional counterions were needed.

The YQNPDGSQA peptide was simulated using three different electrostatic protocols. (I) Particle mesh Ewald (PME) method.[27] An 8 Å cutoff for the real space force contributions and 1.2 Å grid spacing for the Fourier transform in the reciprocal space were used, with fourth-order cubic interpolations for the off-grid positions. (II) Generalized reaction field (GRF) method as implemented by Tironi et al.[28] The dielectric constant of the medium outside an 8 Å cutoff distance was assumed to be 80, which is appropriate for liquid water under ambient conditions. (III) Straight cutoff method, in which contributions of electrostatic energy from pairs of particles separated by distances larger than 8 Å were neglected. The two control peptides were simulated using the GRF method treatment of electrostatics, with the same parameters as for the YQNPDGSQA peptide.

Molecular dynamics simulations were performed according to the replica exchange algorithm,[37−40] starting from random extended coil conformations. The replicas were considered at temperatures exponentially spaced between 280 K and a maximum temperature T_{max} and exchanges of replicas at adjacent temperatures were attempted every 500 simulation steps. The same time interval was used to periodically save atomic coordinates. The parameters used in the simulations are summarized in Table 1.

The first 10 ns of each of these simulations was treated as the equilibration phase and was discarded from the conformational analysis. All the simulations were performed using a parallel version of the GROMACS software.[41−43] During the simulations, covalent bonds of the water molecules were held constant by the SETTLE algorithm.[44] The bonds involving hydrogens of the peptide were constrained according to LINCS protocol,[45] permitting use of a time step of 2 fs. Nonbonded Lennard-Jones interactions were tapered starting at 7 Å and extending to 8 Å cutoff. Neighbor lists for the nonbonded interactions were updated every 10 simulation steps. The

TABLE 1: Parameters of the Replica Exchange Simulations Performed in the Present Work

simulated system	replicas	$T_{min} - T_{max}$ (K)	simulation time for data collection (ns)	acceptance ratio (%)
β-peptide, PME	20	280−540	50	7−40
β-peptide, GRF				10−40
β-peptide, cutoff at 8 Å				10−35
control 1, GRF	26	280−560	40	15−44
control 2, GRF	24	280−580	−	13−43

temperature was controlled during the simulations using the Nose−Hoover algorithm[46] with a 0.05 ps time constant.

The principal component analysis method[47,48] was used to analyze the conformational ensembles generated in simulations. In this approach, a covariance matrix **C** for the deviations of $3N$ atomic coordinates around their average values is constructed:

$$C_{ij} = \langle (x_i - \langle x_i \rangle)(x_j - \langle x_j \rangle) \rangle, \quad i, j = 1, 3N \tag{1}$$

after aligning the analyzed conformations to a reference structure $\mathbf{x}_{ref}$. The covariance matrix is then diagonalized to determine its eigen values λ_i and the corresponding matrix of eigen vectors **R**. The eigen vectors, or principal modes, can be treated as new variables that describe global, collective motions that the studied system can undergo. For better visualization of the generated data, it is convenient to project the simulation trajectories onto principal components $p_i(t)$:

$$\boldsymbol{p}(t) = \mathbf{R}^T(\mathbf{x}(t) - \langle \mathbf{x} \rangle) \tag{2}$$

Projections in the first few principal components, p_i, $i = 1, 2, 3$, provide the best possible views of the conformational space and are most suitable for decomposing the entire conformational space into distinct classes of structures, or clusters.[48] Here, we use two-dimensional projections onto the first two components, *PC*1 and *PC*2.

3. Results

3.1. YQNPDGSQA: β-Hairpin Forming Peptide. The main peptide studied in this work is the YQNPDGSQA peptide, designed by Blanco et al.[29] Mutating the SWRY residues of the 15−23 fragment of α-amylase inhibitor Tendamistat (PDB code 1HOE) into NPDG led to a peptide with enhanced turn-forming propensities and NOEs compatible with a β-hairpin structure. To probe the effects of different electrostatic treatments, three replica exchange molecular dynamics simulations were performed using particle mesh Ewald (PME), generalized reaction field (GRF) and straight cutoffs, as described in the Methods section.

The results of these simulations are displayed in Figure 1. This figure shows a two-dimensional representation of the conformational space (a free energy map), projected onto the first two principal components *PC*1, *PC*2 at $T = 280$ K. These maps indicate that all three methods of treating the electrostatic interactions produce a minimum at (PC1 = −4.2, PC2 = −1.0). For the PME and the reaction field simulations, this minimum is the *global* minimum, i.e., it represents the most statistically significant conformations. We demonstrated in our previous publication[49] that these conformations are β-hairpins, in agreement with experiment. A representative native β-hairpin is shown in Figure 2a. The β-hairpin topology of this conformation is immediately apparent from the characteristic network of interstrand hydrogen bonds that are formed between backbone oxygens and nitrogens.

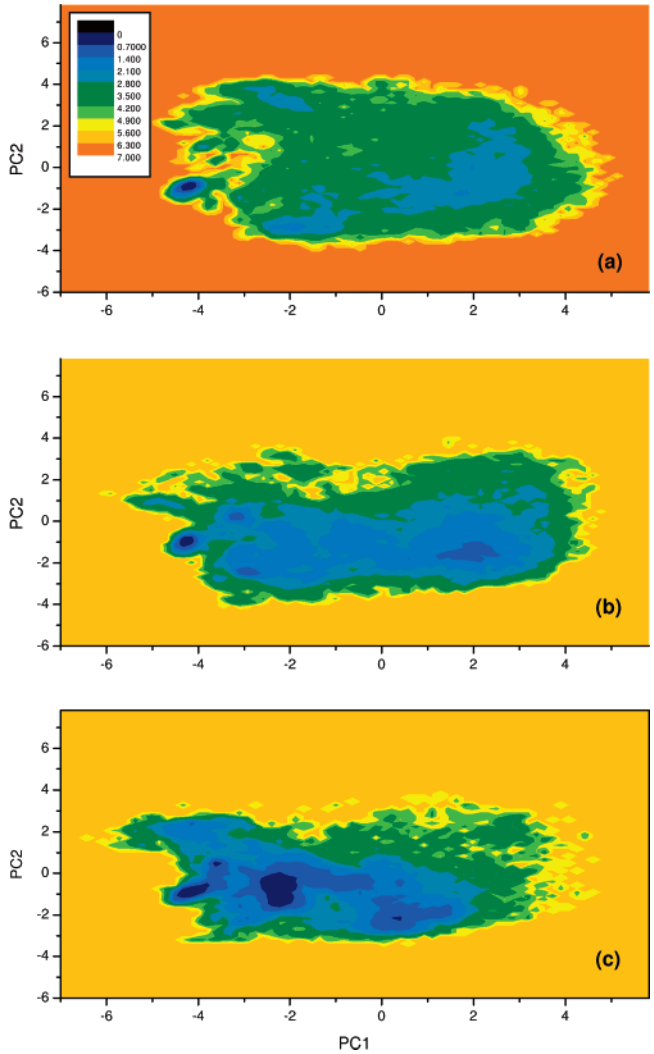

Figure 1. Free energy map of YQNPDGSQA computed as a function of the first two principal components at $T = 280$ K using (a) PME method,[27] (b) generalized reaction field method,[28] and (c) the conventional cutoff scheme for treating electrostatic interactions. Energies are shown in units of kT. All three maps exhibit a global minimum at (*PC*1 = −4.2, *PC*2 = −1.0) corresponding to β-hairpin conformations. The cutoff scheme produces an additional minimum corresponding to non-β-hairpin conformations at (*PC*1 = −2.2, *PC*2 = −0.35).

The main difference between PME- and reaction field-based results concerns the nature of the (non-β-hairpin) unfolded conformations. As seen from (a) and (b) of Figure 1, the reaction field method produces a significantly different unfolded state ensemble from the one seen in the PME simulations, both in terms of its free energy relative to that of the native state as well as its structure (as judged from the two-dimensional representation).

While the PME and reaction field approaches yielded a single free energy minimum, the straight cutoff method produces an additional free energy minimum located at (PC1 = −2.2, PC2 = −0.35). This additional minimum corresponds to non-β-hairpin conformations which strongly compete with the formation of the native β hairpins at low temperatures. A representative of these low-energy, non-native conformations, shown in Figure 2b, displays a loopike structure, stabilized in part by a hydrogen bond between the two charged termini.

On the basis of the fact that experimentally,[29] the YQNPDGSQA peptide forms a unique stable β-hairpin, we conclude

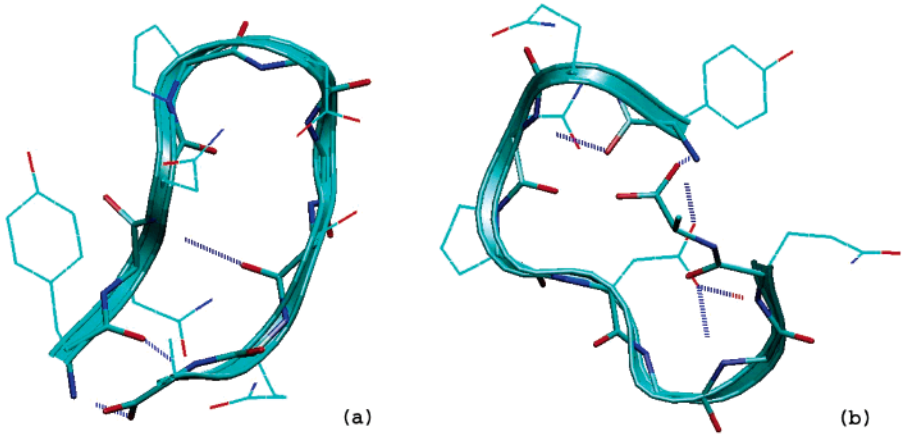

Figure 2. Representative conformation of (a) the native β-hairpin observed in all three simulations of YQNPDGSQA and (b) the additional free energy minimum seen in the cutoff simulations (b).

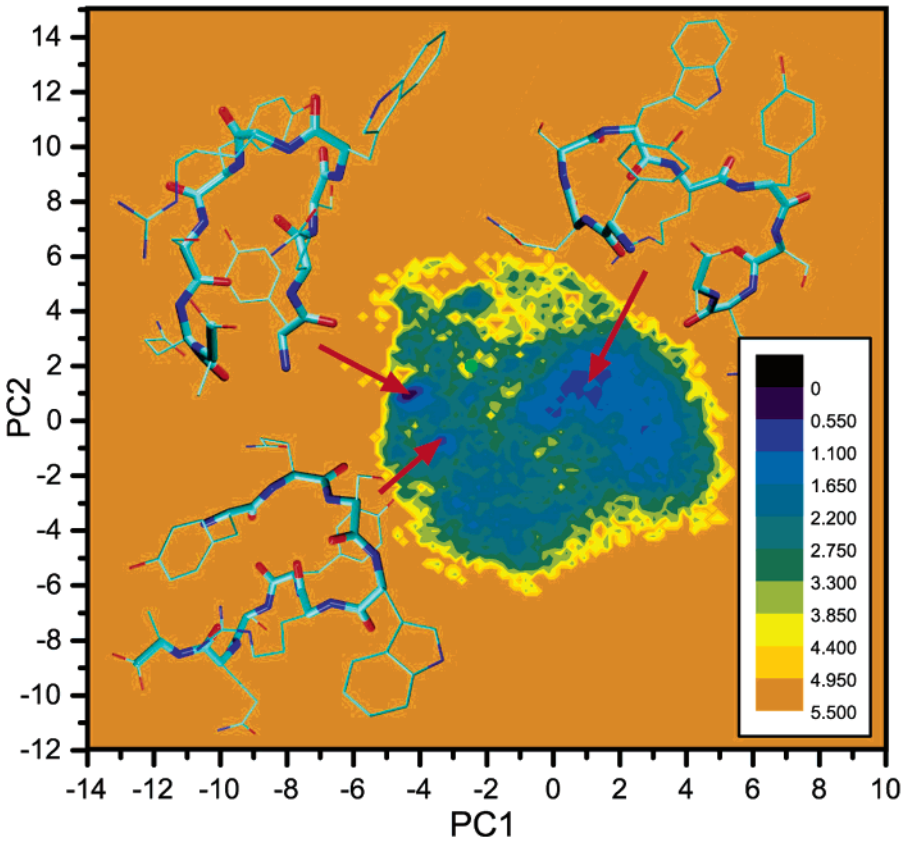

Figure 3. Free energy map of the 15−23 fragment of Tendamistat (YQSWRYSQA) projected on the first two principal coordinates at $T = 280$ K (with GRF treatment of electrostatics). The map exhibits three main minima, with only one of them corresponding to β-hairpin conformations. The location of the native β-hairpin (from the intact protein) is shown as a green circle.

that both the PME and reaction field methods produce a qualitatively correct native state for this system. The straight cutoff treatment of electrostatics, on the other hand, yields results that are inconsistent with experiment, since more than one dominant minimum appears in the free energy map. We note that the use of the replica exchange enhanced sampling technique was critical to reach this conclusion. Starting a simulation from the native β-hairpin conformation and running conventional short constant temperature simulations (on the order of a few nanoseconds) would be insufficient to unfold the peptide and expose the additional free energy minimum present in the straight cutoff approach.

3.2. Control Peptide 1: 15−23 Fragment of the α-Amylase Inhibitor Tendamistat. To further validate the use of the reaction field methods as a viable protocol to identify the low-energy conformations of biomolecules, we tested the GRF approach on two control peptides. The first control peptide studied is the wild-type 15−23 fragment of the α-amylase inhibitor Tendamistat, YQSWRYSQA. This peptide was used in the experiments of Blanco et al.[29,50] to elucidate the role of turn-favoring sequences such as NPDG in stabilizing β-hairpin conformations. As part of the protein, this segment adopts a β-hairpin conformation; however, cleaving the peptide from the protein strongly destabilizes this β-hairpin structure, leading to the transient formation of additional β-turn conformations.[50,29]

The free energy map for this peptide is plotted in Figure 3 at $T = 280$ K as a function of the first two principal components. A mutated version of the native β-hairpin shown in Figure 2a

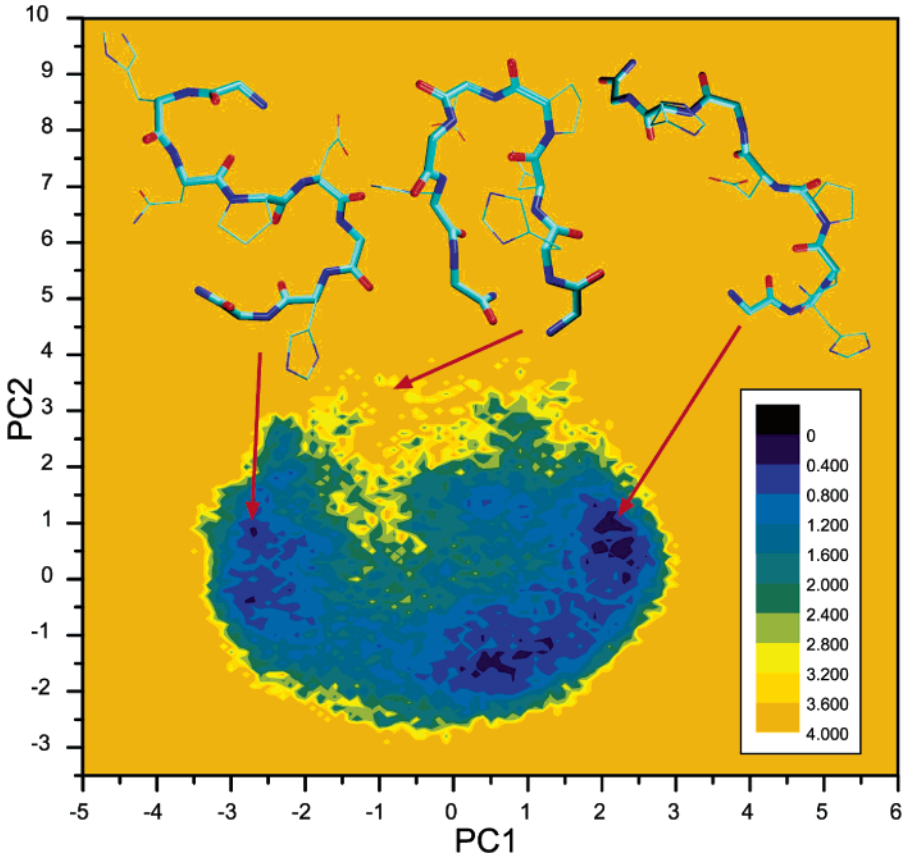

Figure 4. Free energy map of the GHNPDGHG-NH_2 peptide projected on the first two principal coordinates at $T = 280$ K (with GRF treatment of electrostatics). The map exhibits two main minima corresponding to non-β conformations. The reference β-hairpin engineered through mutation and energy minimization of the native state (depicted in Figure 2a) corresponds to a region of high free energy.

which matches the sequence of the present peptide, was used as the reference system for the principal component analysis. While the specific appearance of Figure 3 will be influenced by the choice of reference state, we verified that the conclusions drawn are reference-system independent. The free energy map depicted in Figure 3 shows three equally populated minima, with representative structures belonging to these minima displayed in this figure. Only one of these conformations has a β-hairpin topology, with the other two corresponding to non-β conformations. The observed β-hairpin structure differs by more than 2 Å in C_α RMSD from both the β hairpin of YQNPDGSQA as well as the native β-hairpin present in the full length Tendamistat. The location of the latter is shown as a reference as a green circle in Figure 3. Hence, in agreement with experiment, our REX simulations using a GRF treatment of electrostatics indicate that the 15−23 fragment of Tendamistat does not form a unique stable β-hairpin conformation.

3.3. Control Peptide GHNPDGHG-NH_2. The second control peptide studied, GHNPDGHG-NH_2, is another mutated fragment of the original β-hairpin forming peptide designed by Blanco et al.[29] This peptide maintains the central segment NPDG (which possesses high turn-favoring propensity), and was designed to study the effects of the flanking residues (GLY and HIS) on the stability of β hairpins. Experimentally,[29] this peptide does not form stable β hairpins. Replica exchange molecular dynamics simulations with GRF were performed as described in the Models and Methods section.

As in the case of the first control peptide, a special β-hairpin conformation was engineered from the native state shown in Figure 2a through mutation and subsequent energy minimization to serve as the reference state for the PCA analysis. The results of this analysis are given in Figure 4 which shows the free energy map computed as a function of the first two principal components at $T = 280$ K. The free energy surface displays two "localized" local minima and one broad local minimum. Conformations belonging to the localized minima are shown in Figure 4. None of these conformations possess β-hairpin structure. Conformations that correspond to the broad free energy minimum consist of extended random coils (and are hence not shown in the figure). The location and structure of the mutationally engineered β-hairpin is also given in Figure 4. The coordinates of this conformation correspond to a region of high free energy, and this hairpin will not be populated to a significant extent, in agreement with experimental observations.[29]

4. Discussion and Conclusions

The description of electrostatic interactions in computer simulations has been a vigorous area of research over the last two decades.[15,16] Because of their long-range nature, the evaluation of electrostatic interactions is intrinsically difficult, and a proper representation of all contributions, costly. Much of the research in this field has focused on developing simplified schemes that allow for a more rapid computation of long-range forces. Efficient algorithms are of essence for the study of large systems, (such as biomolecules in explicit solvent); however, approximate treatments of electrostatics must be thoroughly tested to ensure that accuracy is not sacrificed for speed.

The earliest treatments of electrostatics involved a simple truncation of the long-range interactions for distances greater than a given cutoff. It has been long recognized[7,15,17,18] that this straightforward cutoff scheme can cause structural distortions and severely impact protein dynamics. Explicit solvent simula-

tions by Smith and Pettitt[17] on a pentapeptide and salt ions, for instance, revealed that a 7−8 Å cutoff-based switching function is inadequate to simulate the interaction of ions with biomolecules. Similarly, simulations of a 17-residue α-helical peptide by Schreiber and Steinhauser[18,19] indicate that cutoffs as large as 14 Å lead to unstable trajectories over 1 ns simulation times. On a similar time scale, a 9-Å charge group-based cutoff scheme was seen to lead to a clear breakup of DNA and RNA structures in a more recent study by Cheatham et al.,[22] while simulations of HIV-1 protease by York et al.[20] did not converge on an even shorter scale of 300 ps. Most recent failures of the cutoff-based methods for treating electrostatic interactions in biological systems include simulations of the β3 peptide by Monticelli and Colombo[16] and those of lipid bilayers by Patra et al.[51] and Anezo et al.[52] We note that a number of other papers[,22,25,26,53] have reported a successful application of cutoff-based methods in biomolecular simulations. For instance, simulations of myoglobin by Steinbach and Brooks[53] demonstrated that group- and atom-based shifting cutoffs of 12 Å reasonably well approximate simulations where no cutoffs were used. The performance of cutoff-based methods was also found to be satisfactory in simulations of DNA segments,[26] immunoglobulin G (IgG) dimer[25] and ubiquitin.[22,23] Additionally, simulations of *Escherichia coil* thioredoxin protein, confined in a droplet of water,[54] showed only small RMS deviation from the crystal structure, with weak dependence on the particular cutoff scheme used (ranging from 8 to 14 Å and coupled with various switching methods). The importance of using proper potential switching/smoothing techniques was also emphasized in work by Daggett et al.[55] Emerging from these studies is the following general consensus regarding the applicability of cutoff methods for treating electrostatic interactions: (a) the larger the cutoff the better, (b) noncharged systems are usually better handled by cutoff methods than charged ones, and (c) clever switching/shifting techniques may significantly improve the accuracy of the method.[53]

A second, more sophisticated, although still approximate, treatment of electrostatics involves a continuum-based reaction field approach. In contrast to the straight cutoff methods, the performance of this approach in the context of biomolecular simulations has not been extensively investigated, with the majority of studies focusing on solvated ions.[56,57] A recent study on a guanidinium and acetate pair solvated in water indicated that, compared to the Ewald approach, the reaction field method performed better with increasing cutoff radius R_c, with R_c = 12 Å giving satisfactory agreement for the inter-ionic potential of mean force computed using the two methods.[56] In a more recent study, the Ewald summation and reaction field-based methods were shown to be equivalent in the limit of an infinite cutoff.[22] The few studies on biomolecules[24,58,59] include simulations of ubiquitin crystals[24] in which it was found that reaction field and Ewald summation methods did not differ much in their ability to reproduce the crystallographic structure. Similarly, a recent study on porcine procarboxypeptidase B (ADBp) concluded that both methods appear well suited for the simulation of highly charged globular proteins in explicit solvent.

The above-described simulations geared at testing the reliability of straight cutoff and reaction field treatments of electrostatic interactions all involved short (relative to folding time), constant temperature simulations launched from a known native state of the biomolecule. The simulations presented in this paper also seek to evaluate the accuracy of these methods; however, the essential novelty of our work is that we employ a sampling technique that allows access to areas of conformational space that would remain obscured in conventional simulations. A serious potential danger associated with short, constant temperature simulations as a means for assessing the validity of a particular truncation scheme is that such simulations sample only local regions of the conformational space near the initial conformations. By tailoring the methods to improve local agreement with experiment around a given structure, it is possible that these schemes may inadvertently introduce stable conformations in other parts of the conformational space. Should these states be separated by high barriers, insurmountable on time scales of 1−10 ns, these states will not be visited in conventional simulations. Our replica exchange molecular dynamics simulations on a β-forming peptide reveal that an 8 Å atom-based cutoff method results in the creation of an additional free-energy minimum that corresponds to non-β structures, without affecting the population of the main β-hairpin basin to any significant extent. This key finding exposes both the deficiency of a straight cutoff electrostatics truncation scheme, in line with the reports discussed above,[16−20,22] and illustrates the importance of using a simulations methodology that allows consideration of the entire conformational space when assessing the accuracy of different electrostatic treatments. Our replica exchange simulations using both PME and GRF methods, on the other hand, are both capable of reproducing the single, lowest, free energy minimum corresponding to the experimentally determined β-hairpin. Additional tests on two control peptides further establish the GRF method as both an accurate and efficient technique to treat the electrostatic interactions of peptides. A GRF-based approach emerges as a viable computational protocol for the study of large biomolecules for which a PME treatment would be prohibitively costly.

Acknowledgment. Support from the National Science Foundation (CAREER MCB 0133504), the David and Lucile Packard Foundation, and the A. P. Sloan Foundation are gratefully acknowledged. Simulations were performed using the computational resources of the California NanoSystems Institute (NSF Grant CHE-0321368).

References and Notes

(1) Hansson, T.; Oostenbrink, C.; van Gunsteren, W. F. *Curr. Opin. Struct. Biol.* **2002**, *12*, 190−196.
(2) Karplus, M.; McCammon, J. A. *Nat. Struct. Biol.* **2002**, *9* (9), 646−652.
(3) Snow, C. D.; Sorin, E. J.; Rhee, Y. M.; Pande, V. S. *Annu. Rev. Biophys. Biomol. Struct.* **2005**, *34*, 43−69.
(4) Gnanakaran, S.; Nymeyer, H.; Portman, J.; Sanbonmatsu, K. Y.; Garcia, A. E. *Curr. Opin. Struct. Biol.* **2003**, *13*, 168−174.
(5) Onuchic, J. N.; Luthey-Schulten, Z.; Wolynes, P. G. *Annu. Rev. Phys. Chem.* **1997**, *48*, 545−600.
(6) Shea, J.-E.; Brooks, C. L., III. *Annu. Rev. Phys. Chem.* **2001**, *52*, 499−535.
(7) Cheatham, T. E., III; Brooks, B. R. *Theor. Chem. Acc.* **1998**, *99*, 279−288.
(8) Gilson, M. K. *Curr. Opin. Struct. Biol.* **1995**, *5*, 216−223.
(9) Price, D. J.; Brooks, C. L., III. *J. Comput. Chem.* **2002**, *23*, 1045−1057.
(10) Hu, H.; Elstner, M.; Hermans, J. *Proteins: Struct., Funct., Genet.* **2003**, *50*, 451−463.
(11) Mu, Y.; Kosov, D. S.; Stock, G. *J. Phys. Chem. B* **2003**, *107*, 5064−5073.
(12) Zaman, M. H.; Shen, M.-Y.; Berry, R. S.; Freed, K. F.; Sosnick, T. R. *J. Mol. Biol.* **2003**, *331*, 693−711.
(13) Shirts, M. R.; Pitera, J. W.; Swope, W. C.; Pande, V. S. *J. Chem. Phys.* **2003**, *119*, 5740−5761.
(14) Kastenholz, M. A.; Hünenberger, P. H. *J. Phys. Chem. B* **2004**, *108*, 774−788.
(15) Loncharich, R. J.; Brooks, B. R. *Proteins: Struct., Funct., Genet.* **1989**, *6*, 32−45.
(16) Monticelli, L.; Colombo, G. *Theor. Chem. Acc.* **2004**, *112*, 145−157.

(17) Smith, P. E.; Pettitt, B. M. *J. Chem. Phys.* **1991**, *95*, 8430−8441.
(18) Schreiber, H.; Steinhauser, O. *Biochemistry* **1992**, *31*, 5856−5860.
(19) Schreiber, H.; Steinhauser, O. *Chem. Phys.* **1992**, *168*, 75−89.
(20) York, D. M.; Wlodawer, A.; Pedersen, L. G.; Darden, T. A. *Proc. Natl. Acad. Sci. U.S.A.* **1994**, *91*, 8715−8718.
(21) York, D. M.; Darden, T. A.; Pedersen, L. G. *J. Chem. Phys.* **1993**, *99*, 8345−8348.
(22) Cheatham, T. E., III; Miller, J. L.; Fox, T.; Darden, T. A.; Kollman, P. A. *J. Am. Chem. Soc.* **1995**, *117*, 4193−4194.
(23) Fox, T.; Kollman, P. A. *Proteins: Struct., Funct., Genet.* **1996**, *25*, 315−334.
(24) Walser, R.; Hünenberger, P. H.; van Gunsteren, W. F. *Proteins: Struct., Funct., Genet.* **2001**, *44*, 509−519.
(25) Krol, M. *J. Mol. Model.* **2003**, *9*, 316−324.
(26) Norberg, J.; Nilsson, L. *Biophys. J.* **2000**, *79*, 1537−1553.
(27) Essmann, U.; Perera, L.; Berkowitz, M. L.; Darden, T.; Lee, H.; Pedersen, L. G. *J. Chem. Phys.* **1995**, *103*, 8577−8593.
(28) Tironi, I. G.; Sperb, R.; Smith, P. E.; van Gunsteren, W. F. *J. Chem. Phys.* **1995**, *102*, 5451−5459.
(29) Blanco, F. J.; Jimenez, M. A.; Herranz, J.; Rico, M.; Santoro, J.; Nieto, J. L. *J. Am. Chem. Soc.* **1993**, *115*, 5887−5888.
(30) Constantine, K. L.; Mueller, L.; Andersen, N. H.; Tong, H.; Wandler, C. F.; Friedrichs, M. S.; Bruccoleri, R. E. *J. Am. Chem. Soc.* **1995**, *117*, 10841−10854.
(31) Friedrichs, M. S.; Stouch, T. R.; Bruccoleri, R. E.; Mueller, L.; Constantine, K. L. *J. Am. Chem. Soc.* **1995**, *117*, 10855−10864.
(32) Constantine, K. L.; Friedrichs, M. S.; Stouch, T. R. *Biopolymers* **1996**, *39*, 591−614.
(33) Wu, X.; Wang, S.; Brooks, B. R. *J. Am. Chem. Soc.* **2002**, *124*, 5282−5283.
(34) Wu, X.; Brooks, B. R. *Biophys. J.* **2004**, *86*, 1946−1958.
(35) Kaminski, G. A.; Friesner, R. A.; Tirado-Rives, J.; Jorgensen, W. L. *J. Phys. Chem. B* **2001**, *105*, 6474−6487.
(36) Jorgensen, W. L.; Chandrasekhar, J.; Madura, J. D.; Impey, R. W.; Klein, M. L. *J. Chem. Phys.* **1983**, *79*, 926−935.
(37) Sugita, Y.; Okamoto, Y. *Chem. Phys. Lett.* **1999**, *314*, 141−151.
(38) Okamoto, Y. *J. Mol. Graphics Model.* **2004**, *22*, 425−439.
(39) Garcia, A. E.; Onuchic, J. N. *Proc. Natl. Acad. Sci. U.S.A.* **2003**, *100*, 13898−13903.
(40) Pitera, J. W.; Swope, W. *Proc. Natl. Acad. Sci. U.S.A.* **2003**, *100*, 7587−7592.
(41) Lindahl, E.; Hess, B.; van der Spoel, D. *J. Mol. Model.* **2001**, *7*, 306−317.
(42) Berendsen, H. J. C.; van der Spoel, D.; van Drunen, R. *Comput. Phys. Commun.* **1995**, *91*, 43−56.
(43) Replica exchange facility for GROMACS was written by Luca Monticelli and Walter Ash, University of Calgary.
(44) Miyamoto, S.; Kollman, P. A. *J. Comput. Chem.* **1992**, *13*, 952−962.
(45) Hess, B.; Bekker, H.; Berendsen, H. J. C.; Fraaije, J. G. E. M. *J. Comput. Chem.* **1997**, *18*, 1463−1472.
(46) Nosé, S. *Prog. Theor. Phys.* **1991**, *103*, 1−46.
(47) van der Spoel, D.; Lindahl, E.; Hess, B.; van Buuren, A. R.; Apol, E.; Meulenhoff, P. J.; Tieleman, D. P.; Sijbers, A. L. T. M.; Feenstra, K. A.; van Drunen, R.; Berendsen, H. J. C. *Gromacs User Manual*, version 3.2; http://www.gromacs.org, 2004.
(48) Jolliffe, I. T. *Principal Component Analysis*; Springer-Verlag: New York, Berlin, Heidelberg, Tokyo, 1986.
(49) Baumketner, A.; Shea, J.-E. *Theor. Chem. Acc.* **2005**, submitted.
(50) Blanco, F. J.; Jimenez, M. A.; Rico, M.; Santoro, J.; Herranz, J.; Nieto, J. L. *Eur. J. Biochem.* **1991**, *200*, 353−358.
(51) Patra, M.; Karttunen, M.; Hyvonen, M. T.; Falck, E.; Lindqvist, P.; Vattulainen, I. *Biophys. J.* **2003**, *84*, 3636−3645.
(52) Anezo, C.; de Vries, A. H.; Holtje, H. D.; Tieleman, D. P.; Marrink, S. J. *J. Phys. Chem. B* **2003**, *107*, 9424−9433.
(53) Steinbach, P. J.; Brooks, B. R. *J. Comput. Chem.* **1994**, *15*, 667−683.
(54) Garemyra, R.; Elofsson, A. *Proteins: Struct., Funct., Genet.* **1999**, *37*, 417−428.
(55) Beck, D. A. C.; Armen, R. S.; Daggett, V. *Biochemistry* **2005**, *44*, 609−616.
(56) Rozanska, X.; Chipot, C. *J. Chem. Phys.* **2000**, *112*, 9691−9694.
(57) Peter, C.; van Gunsteren, W. F.; Hünenberger, P. H. *J. Chem. Phys.* **2003**, *119*, 12205−12223.
(58) Tieleman, D. P.; Hess, B.; Sansom, M. S. P. *Biophys. J.* **2002**, *83*, 2393−2407.
(59) Gargallo, R.; Hünenberger, P. H.; Aviles, F. X.; Oliva, B. *Protein Sci* **2003**, *12*, 2161−2172.